ISSN:2229-6107

INTERNATIONAL JOURNAL OF PURE AND APPLIED SCIENCE & TECHNOLOGY

E-mail :
editor.ijpast@gmail.com
editor@ijpast.in

www.ijpast.in

INTERNATIONAL JOURNAL OF PURE AND APPLIED SCIENCE & TECHNOLOGY
IJPAST

ISSN 2229-6107 www.ijpast.in

Vol 13,Issuse 2.May 2023

A NOVEL CONTROL SCHEME FOR WIND TURBINE DRIVEN DFIG INTERFACED TO UTILITY GRID USING MPC AND P&O TECHNIQUE

[1]I. ROHINI, [2]K. SOWBHAGYA LAKSHMI,[3]R. YOCHANA,[4]V NAGA SUSHMA

ABSTRACT

This article deals with a phase-locked loop (PLL)- based novel control for wind turbine driven doubly fed induction generator interfaced to utility grid with a battery energy storage (BES) connected at the dc link. The control of grid-side converter (GSC) is modified to export/import constant power to/from the grid. The state of charge of BES helps in deciding the reference export power to the grid apart from the manual selection using averaged wind power in a particular period of time. An off maximum power point tracking logic is incorporated in the rotor-side converter (RSC) control to operate the BES within its constraints and, moreover, to feed constant power to the grid. In addition, the energy management scheme of the system is presented in the form of flowchart for both exporting and importing power to/from the grid. The RSC and GSC have taken care of unity power factor operation at stator terminals and to mitigate harmonics and grid currents balancing, respectively. The system performance is found robust as the PLL response is not affected even under grid voltages with dc offset. The system is modeled and simulations are carried out in MATLAB using SimPowerSystems tool box. Moreover, the control scheme performance is comparedwith conventional control algorithms both in terms of PLLand converter controls.To validate the effectiveness of the control scheme, a prototype of the system is developed. Test results demonstrate the satisfactory performance of the system under various operating conditions.

INTRODUCTION

Both economic and demographic expansion contribute to the continuously rising need for power. Furthermore, traditional electricity generating causes pollution, global warming, and depletes fossil fuel reserves. Improvements in power electronics technology have also contributed to this trend toward using renewable energy sources like wind to generate electricity. Due to its benefits, such as lower converter rating and variable speed operation, the doubly fed induction generator (DFIG) is a viable option for getting the most power out of the wind [1]. The wind-powered DFIG may function both independently and in grid-connected configurations. An important part of a grid-connected DFIG system is the ability to smooth out power fluctuations and calculate grid reference power. The BES is utilized to provide consistent electricity to the grid regardless of wind speeds. The grid power may also be smoothed using the techniques described in [2]-[4]. The authors of [2] explain how a variable-frequency transformer may be used to smooth out power outages. The best way to choose capacitors and inductors, however, is glossed over. There is also no way to put the stated plan into action. Superconducting magnetic energy storage for smoothing out power fluctuations on the grid is given by the authors of [3]. However, the theoretical analysis of the system is not verified by test data. To mitigate power fluctuations on the grid, an adjusted maximum power point tracking (MPPT) method is presented in [4].

However, when the greatest wind power output is more than or equal to the grid reference power, this strategy works effectively. For the reason that if the peak production is lower than the grid reference power, power smoothing will not occur. Furthermore, hardware implementation details are not provided for this technique. The writers of [1], [5], and [6] have described the DFIG's relationship with the power grid. However, exporting reference power calculations are left out of the discussion. If one's control is based on a voltage-oriented reference frame, another crucial block is the phase-locked loop (PLL), which generates the synchronous angle.

[1]ASSISTANT PROFESSOR, [2,3&4] UG SCHOLAR

DEPARTMENT OF EEE,

MALLA REDDY ENGINEERING COLLEGE FOR WOMEN, HYDERABAD

If a DC offset is applied to the input of a phase-locked loop, the output frequency and phase angle will be incorrect. Numerous PLL architectures may be discovered in the scholarly works [7], [8]. Some of these, however, are complicated while others hinder the dynamic performance. In order to get the most out of the setup, it is crucial to maximize wind power extraction. Several wind MPPT strategies have been documented in the literature as means of accomplishing this goal [9], [10]. Here, maximum power point tracking (MPPT) control based on the tip speed ratio is used to get the most out of the wind. Wind-powered DFIG with a battery energy storage system (BES) interface is the focus of this study. The following are examples of characteristics of control that this work improves upon.

In order to export regulated electricity to the grid based on averaged wind power and state of charge (SOC) of the BES, as well as user selection of export or import, the control of the grid side converter (GSC) is adjusted.

To get the most energy out of the wind, the rotor side converter (RSC) is modulated to meet the DFIG's reactive power needs and to regulate the rotor's rotational speed.

• The BES is used to keep the grid's regulated electricity flowing at all times, regardless of the wind.

• The DC offset at the input is suppressed by using a phase-locked loop (PLL), which allows for effective GSC and RSC regulation.

• Harmonic-free and balanced grid-side currents in accordance with the IEEE 519 standard are achieved with the suggested control for GSC. An experimental prototype of a DFIG with a grid interface and a battery energy storage system is built. Wind speed, export/import grid power, load, and nonlinear load coupled at the point of common coupling (PCC) are only some of the situations evaluated.

SETTING UP THE SYSTEM

Connected to the utility grid, the DFIG-based wind energy conversion system (WECS) is shown in Fig. 1. The DFIG's RSC, GSC, and BES all have DC links to back-to-back converters. The wind turbine's power capture and the rotor power coefficient (Cp) are listed in [11]. A wind turbine with a 12 m/s rating is developed in this study.

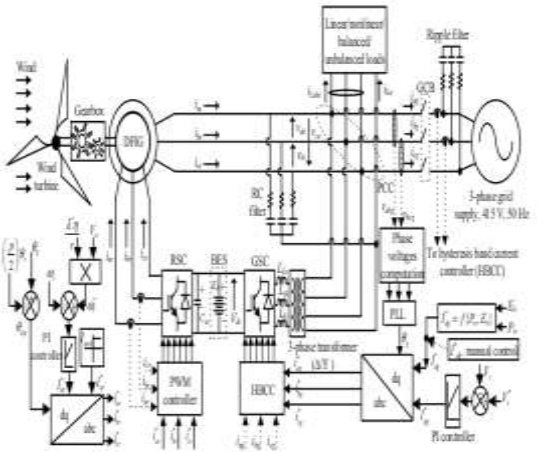

Fig. 1. Utility grid-interfaced wind driven DFIG.

wind speed, for a 5 kVA rated DFIG. The tip-speed ratio MPPT technique generates reference rotor speed, which depends on step-up gear ratio (), optimal tip speed ratio (————————————————*) and r, as shown in Fig. 1. The system parameters and power ratings of different components, are computed using a procedure based on the literature reported in [12]. The design parameters of different components of proposed scheme, are mentioned in Table-I.

TABLE I. SYSTEM PARAMETERS AND POWER RATINGS

Doubly Fed Induction Generator (DFIG)
Rating: 5 kVA, stator voltage: 400 V, stator frequency: 50 Hz, number of poles: 4, stator winding connection: Y, R_s: 1.32 Ω, R_r: 1.708 Ω, L_m: 219 mH, L_{ls}: 6.832 mH, L_{lr}: 6.832 mH, inertia =0.1878 kg-m^2, stator current: 12 A, rotor voltage: 200 V, rotor current: 18 A, rotor connection: Y.
Wind Turbine
Turbine rotor length, r=2.08 m, gear ratio η=4.36, optimal tip speed ratio, λ^*=8.1, rotor power coefficient, C_p=0.48, rated wind speed=12 m/s, minimum and maximum rotor speeds of DFIG, ω_{rmin}=110 rad/s and ω_{rmax}=204 rad/s.
Battery Energy Storage (BES)
E_{bi}: 240 V, E_{bmax}: 270 V, E_{bmin}: 210V; 20 units of 12 V, 7 AH batteries, 5 kWh.
DC Machine
Capacity: 5 kW, field voltage: 230 V, armature voltage: 230 V, R_a: 1.3 Ω, R_f: 220 Ω, L_f: 7.5 mH, L_a: 7.2 mH, K_ϕ: 1.3314, rated speed: 1500 rpm, armature current: 21.8 A.
Transformer, Interfacing Inductor and Ripple Filter
3-phase transformer rating: 5 kVA, 50 Hz; Interfacing inductance, L_f=1.2 mH; Resistance and capacitance of RC filter (ripple filter): R= 5 Ω, C=10 μF.
Voltage Source Converters (RSC and GSC)
Rating of GSC: 2.5 kVA; Rating of RSC: 1.615 kVA.

MODELS OF REGULATION

In this study, a voltage-oriented reference frame is used for RSC and GSC control. Therefore, the active power is represented by the d component along the direct axis, and the reactive power by the q component along the quadrature axis. Detailed explanations of the RSC and GSC control systems shown in Fig. 1 are provided below.

1) The Algorithm for Controlling the RSC

The goals of the RSC control are as follows.

• It provides the reactive power needed by DFIG to keep the stator terminals' power factor at unity.

• It regulates rotor speed to harvest the most energy possible from the breeze. Calculating the machine's no-load magnetizing current (Ims0) yields the reference reactive component of rotor current (I * qr).

$$I_{ms0} = I^*_{qr} = \left(\sqrt{\frac{2}{3}}\right)\frac{V_g}{X_m} \quad (1)$$

where Vg equals to 415 V and Xm represents reactance of the machine at base frequency. The active reference current (I * dr), is obtained by comparing reference rotor speed (

---

* r) with actual speed (

---

r) and passing error through the proportional and integral (PI) controller. The mathematical form to estimate I * dr is as follows

$$I^*_{dr(k)} = I^*_{dr(k-1)} + K_{pw}(\omega_{err(k)} - \omega_{err(k-1)}) + K_{iw}\omega_{err(k)} \quad (2)$$

where
Kp

---

and
Ki

---

represent proportional and integral constants of speed controller and

---

err(k) and

---

err(k-1) represent speed error at kth and (k-1)the instants, respectively. By using slip angle (slp), (1) and (2) are transformed to actual ABC quantities (i * ar, i * br and i * cr) and they are compared with the sensed rotor currents (iar, ibr and icr) to generate pulses for RSC, as depicted in Fig. 1. The angle of transformation (slp), is computed from the angle generated from PLL (g) and rotor angle from encoder (r) as,

$$\theta_{slp} = \theta_g - \left(\frac{p}{2}\right)\theta_r$$

where p represents number of poles of the machine

. GSC Control Algorithm the GSC functions to achieve the following objectives.

• It provides the reactive power requirement of the load.

• It regulates the export or import power along the utility grid.

• It helps in power quality improvement in the grid side such as harmonics compensation, unbalanced load compensation, thereby maintaining total harmonic distortion (THD) of PCC voltages and currents within the IEEE 519 standard

The control of GSC is shown in Fig. 1, in which the reference terminal voltage (V* t) and actual voltage (Vt), are compared and the error is passed through PI voltage controller to generate the reactive reference component (I * qg) of grid current. The computation of I * qg is as follows.

$$I^*_{qg(k)} = I^*_{qg(k-1)} + K_{pv}(\delta V_{(k)} - \delta V_{(k-1)}) + K_{iv}\delta V_{(k)} \quad (4)$$

Kpv, Kiv stand for the proportional and integral constants of the PI voltage controller, while V(k)= V* t(k) - Vt(k) is the voltage error at the kth instant. In this study, a novel method, shown in Fig. 1, is presented for automatically generating the active reference current component of grid current (I * dg). The average active power production by DFIG during a certain time period and samples of wind speeds, which vary over time, are used as the basis for the first decision. Second, it's calculated using the battery's state of charge (SOC). If the amount of energy produced is more than the amount used by the reference grid, the excess energy is sent to the battery energy storage system (BES) for charging. The battery's state of charge (SOC) determines whether or not the system should export energy to the utility grid or import energy from it.

RESULTS OF EXPERIMENTS

The suggested control method is verified experimentally using a wind simulator and a DFIG rated at 5 kVA. The DFIG's rotor circuit has a pair of converters—an RSC and a GSC—connected in series. DC link is used to connect the BES. The AC current from the GSC is amplified by a 3-phase /Y transformer and then sent to the PCC, while the neutral line is utilized to power single-phase appliances. A DC shunt motor and buck chopper are used to mimic the wind's movement. Since the DC motor's stator and armature conductors are energized independently, the chopper is used to regulate the motor's torque. Table-I of section-II lists the DFIG, BES, and DC motor experimental parameters. The RSC and GSC control algorithms are implemented in a digital signal processor (dSPACE-1103 and R&D digital controller) with a sampling time of 35 s. Wind speed (Vw), power (Pw), load (PL), GSC (PGSC), rotor (Nr) speed, rotor (ira) current, load (iLa) current, stator (Ps) power, battery (Pb) power, grid (iga) current, and grid reference (PGRef) power are all utilized in the demonstration.

Nonlinear Load Steady-State Performance of the System

Figure 3 depicts the system's steady-state performance under nonlinear load. The voltage and current waveforms of the grid, the load, and the GSC are shown in Figs. 3(a), (b), and (c), respectively. In Fig. 3(d-e), we see the load power and GSC power. The harmonic spectra of the load current, grid current, and GSC current are shown in Figs. 3(f)–(h). The harmonic spectrum of PCC voltage is shown in Fig. 3(i). This demonstrates that even under a nonlinear load state, the THD of both the grid current and the PCC voltage are acceptable.

System Efficiency at Varying Wind Velocities

The dynamic performance of the system at varying wind speeds is shown in Figs. 4-5 (a-d). Waveforms of Vw, Ps, ira, and Pb during transitions from sub synchronous to super synchronous rotor speed are shown in Fig. 4. The waveforms of Vw, Pw, PL, and PGSC are shown in Fig. 5 (a). Constant power is flowing through the grid and the linked load. As may be seen in Fig. 5 (a), wind power rises with increasing wind speed. The additional wind electricity is being sent to BES through GSC. This means that changes in wind power are reflected in GSC output. The waveforms of Vw, Nr, ira, and Ps are shown in Figs. 5(b) and (c). In this case, the rotor speed rises and the rotor current frequency decreases as wind speed increases. Nonetheless, DFIG stator power is enhanced. The dynamic behavior of the system is shown in Fig. 5 (c), which shows the shift from subsynchronous to super synchronous DFIG speed. It is determined that the point at which the rotor current changes to DC is synchronous speed. In Fig. 5 (d), we see examples of the waveforms for Vw, Ps, PGSC, and Pb. Stator power is raised in proportion to wind speed. Due to the stability of grid power, the GSC is used to transfer any unused power from the stator to the battery. The waveform of the battery in Figure 5 (d) demonstrates this clearly.

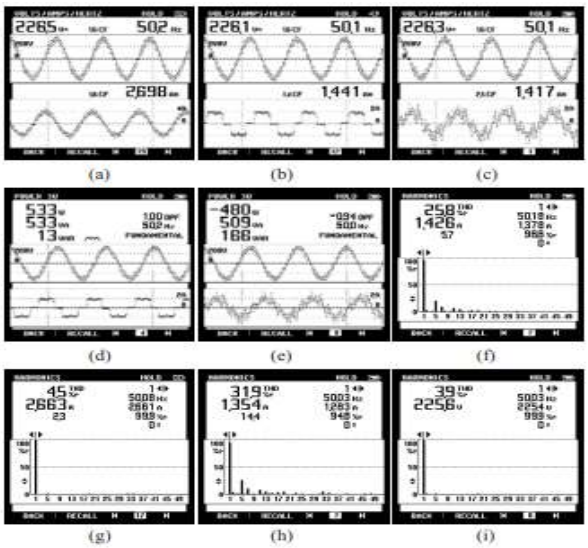

Fig. 3. Experimental waveforms of a system at steady state with nonlinear load (a-c) voltage and current waveforms of grid, load and GSC (d-e) load power and GSC power (f-h) Harmonic spectrum of load, grid and GSC current (I) Harmonic spectrum of PCC voltage.

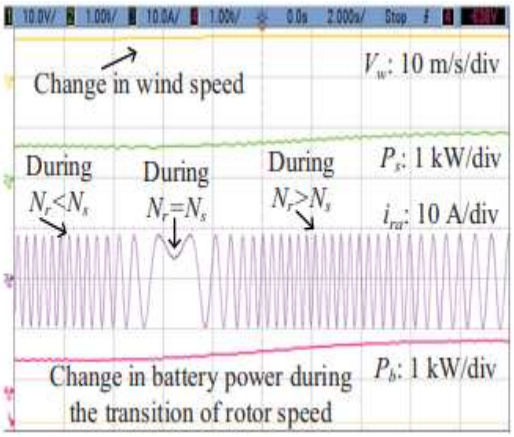

Fig. 4. Response of BES during change in wind speed: Vw, Ps, ira and Pb.

System Performance During Change in Export/Import Grid Reference Power

Figs. 6 (a-c) demonstrate the dynamic performance of the system during changes in export power, import power and transition from export to import, respectively. Fig. 6 (a) depict the waveforms of Pw, PL, PG and PGSC during change in export grid reference power. In this case, wind speed and load,

are kept constant. Therefore, the increase or decrease of export power to the grid is taken care by BES, which reflects in GSC power as shown in Fig. 6 (a). In similar lines, Fig. 6 (b) shows the performance of the system during change in import power from the grid. Fig. 6 (c) depicts the waveforms of PGRef, PG, Ps and PGSC during the transition of reference grid power from exporting to importing. In this scenario, load and wind speed are unaltered. Hence, stator and load powers, are constant. The grid reference power is changed from export to import and it is found that actual

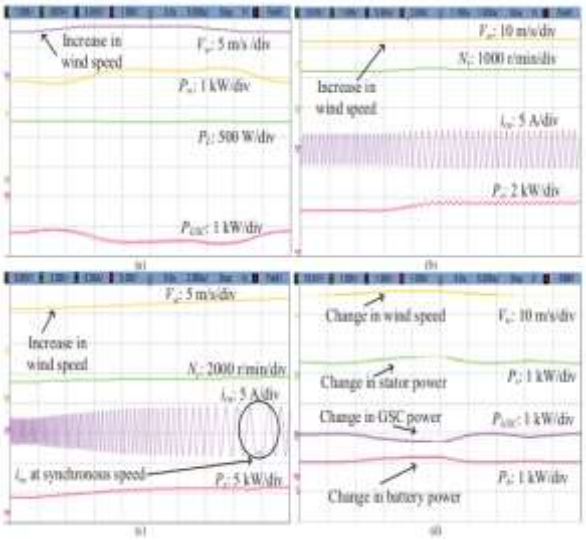

Fig. 5. System performance at variable wind speeds: (a) Vw, Pw, PL and PGSC (b-c) Vw, Nr, ira and Ps (d) Vw, Ps, PGSC and P

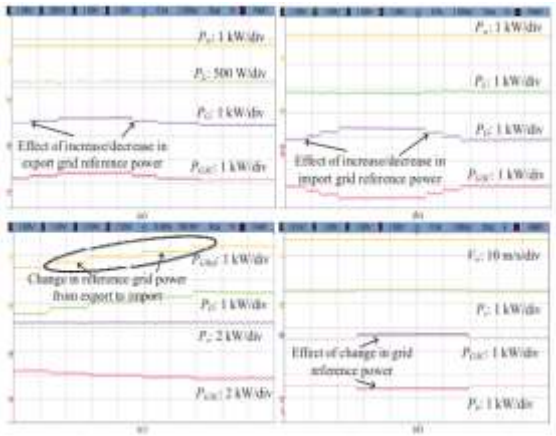

Fig. 6. Dynamic performance of system (a) Change in export grid reference power: Pw, PL, PG and PGSC (b) Change in import grid reference power: Pw, PL, PG and PGSC (c) During transition of reference grid power from exporting to importing: PGRef, PG, Ps and PGSC (d) BES response during change in export grid reference power: Vw, Ps, PGSC and Pb.

Power from the grid (PG) is also adjusted as needed. As shown in Fig. 6 (c), the GSC power is reflective of the variations in grid reference power maintained by BES due to the constant wind speed. BES's reaction to a shift in the export grid's reference power is seen in d) in Fig. 6. At a fixed velocity of wind, it displays the waveforms of Vw, Ps, PGSC, and Pb. Stator power is shown to be constant in Fig. 6(d) due to the constancy of wind speed. According to the battery power waveform, the BES can handle the higher export power. The suggested control for controlling grid power has been implemented, and a manual control has also been performed. During human management of grid reference power at a constant wind speed, as shown in Fig. 7, the performance of the system is shown. Here, BES aids the alterations to the electricity referenced by the grid.

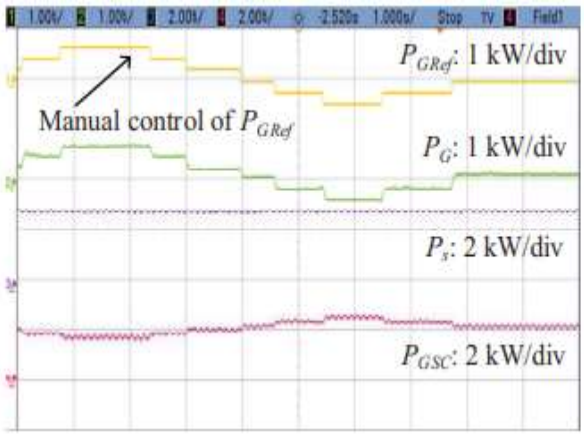

Fig. 7. System performance during manual control of grid reference power: PGRef, PG, Ps and PGSC.

System Performance During Change in Load

Fig. 8 depicts the waveforms of Vw, Pw, PL and PGSC during an increase in load connected at PCC. In this scenario, the wind speed is kept constant and thereby stator power is constant. Moreover, grid reference power is unaltered. Therefore, the increased load demand is met by the BES. Here, the power flows from BES through GSC to the load. Therefore, the GSC power changes with changes in load demand, as shown in Fig. 8.

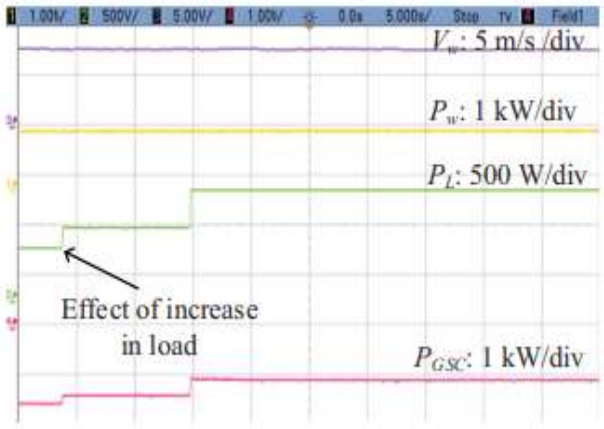

Fig. 8. System performance during increase in load: Vw, Pw, PL and PGSC.

CONCLUSION

A new control approach based on a phase-locked loop (PLL) has been presented for a wind-driven DFIG system with a grid interface and a BES linked through a direct current (DC) connection. To maximize energy harvesting from wind in the face of varying wind speeds, the control system has included the tip-speed ratio MPPT approach. The BES aids in both steady electricity import and export through the grid. The battery is charged when production exceeds consumption and gets discharged when production falls short of demand. The results of the tests show that the GSC is capable of mitigating the harmonics present in the exported and imported power by compensating for the active power reference component provided by the grid. The RSC is also well-managed to ensure that the power factor at the stator terminals is 1. The test findings show that the wind power production system performs well in real-world conditions of varying wind speeds and changing loads. THDs of grid currents-voltages were determined to be acceptable, falling within the range specified by IEEE-519.

REFERENCES

[1] C. Wu and H. Nian, "Stator harmonic currents suppression for DFIG based on feed-forward regulator under distorted grid voltage," IEEE Trans. Power Electron., vol. 33, no. 2, pp. 1211-1224, Feb. 2018.

[2] L. Wang and L. Y. Chen, "Reduction of power fluctuations of a largescale grid-connected offshore wind farm using a variable frequency transformer," IEEE Trans. Sustain. Energy, vol. 2, no. 3, pp. 226-234, July 2011.

[3] X. Y. Xiao, R. H. Yang, X. Y. Chen, Z. X. Zheng, and C. S. Li, "Enhancing fault ride-through capability of DFIG with modified SMES-FCL and RSC control," IET Gener., Transm. & Distrib., vol. 12, no. 1, pp. 258-266, Jan. 2018.

[4] D. Ochoa and S. Martinez, "Fast-frequency response provided by DFIG-wind turbines and its impact on the grid," IEEE Trans. Power Systems, vol. 32, no. 5, pp. 4002-4011, Sept. 2017.

[5] D. Sun, X. Wang, H. Nian, and Z. Q. Zhu, "A sliding-mode direct power control strategy for DFIG under both balanced and unbalanced grid conditions using extended active power," IEEE Trans. Power Electron., vol. 33, no. 2, pp. 1313-1322, Feb. 2018.

[6] X. Wang, D. Sun, and Z. Q. Zhu, "Resonant-based backstepping direct power control strategy for DFIG under both balanced and unbalanced grid conditions," IEEE Trans. Ind. Applicat., vol. 53, no. 5, pp. 4821-4830, Oct. 2017.

[7] G. Chen, L. Zhang, R. Wang, L. Zhang, and X. Cai, "A novel SPLL and voltage sag detection based on LES filters and improved instantaneous symmetrical components method," IEEE Trans. Power Electron., vol. 30, no. 3, pp. 1177-1188, March 2015.

[8] M. Xie, H. Wen, C. Zhu, and Y. Yang, "DC offset rejection improvement in single-phase SOGI-PLL algorithms: Methods review and experimental evaluation," IEEE Access, vol. 5, pp. 12810-12819, 2017.

[9] J. Tian, D. Zhou, C. Su, Z. Chen, and F. Blaabjerg, "Reactive power dispatch method in wind farms to improve the lifetime of power converter considering wake effect," IEEE Trans. Sustain. Energy, vol. 8, no. 2, pp. 477-487, April 2017.

[10] R. Bhattarai, N. Gurung, S. Ghosh, and S. Kamalasadan, "Parametrically robust dynamic speed estimation based control for doubly fed induction generator," IEEE Trans. Ind. Applicat., Early Access.

[11] S. Heier, Grid Integration of Wind Energy Conversion Systems. Hoboken, NJ: Wiley, 1998.

[12] S. Kumar Tiwari, B. Singh, and P. K. Goel, "Design and control of microgrid fed by renewable energy generating sources," IEEE Trans. Ind. Applicat., vol. 54, no. 3, pp. 2041-2050, May-June 2018.